LASER INTERFEROMETER GRAVITATIONAL WAVE OBSERVATORY

LIGO Laboratory / LIGO Scientific Collaboration

LIGO- T050064-00-R *Initial LIGO* 04/23/2005

Thermal Compensation System Description

Stefan Ballmer, Valery Frolov, Ryan Lawrence, William Kells, Gerado Moreno, Ken Mason, David Ottaway, Mike Smith, Cheryl Vorvick, Phil Willems and Mike Zucker

Distribution of this document:
LIGO Science Collaboration

This is an internal working note
of the LIGO Project.

California Institute of Technology
LIGO Project – MS 18-34
1200 E. California Blvd.
Pasadena, CA 91125
Phone (626) 395-2129
Fax (626) 304-9834
E-mail: info@ligo.caltech.edu

Massachusetts Institute of Technology
LIGO Project – NW17-161
175 Albany St
Cambridge, MA 02139
Phone (617) 253-4824
Fax (617) 253-7014
E-mail: info@ligo.mit.edu

LIGO Hanford Observatory
P.O. Box 1970
Mail Stop S9-02
Richland WA 99352
Phone 509-372-8106
Fax 509-372-8137

LIGO Livingston Observatory
P.O. Box 940
Livingston, LA 70754
Phone 225-686-3100
Fax 225-686-7189

http://www.ligo.caltech.edu/

1 Introduction

1.1 Purpose

The purpose of this document is to give a complete description of the Thermal Compensation System (TCS) that has recently been installed on all three LIGO Interferometers. This document includes a design philosophy, step by step description of the layout and some preliminary results.

1.2 Applicable Documents and Drawings

1. Ryan Lawrence "Active Wavefront Correction in Laser Interferometric Gravitational Wave Detectors", PhD Dissertation, LIGO Document P030001-00
2. Ryan Lawrence, David Ottaway, Peter Fritschel and Mike Zucker, " Active correction of beam heating induced phase distortions in optics via external radiative thermal actuation" *Optics Letters*, Vol. 29 (22) pp 2635-2637, 2004
3. Mike Zucker, David Ottaway and Ken Mason, "Thermal Compensation Retrofit for LIGO 1" T030062-03-D
4. Michael Smith, David Ottaway, Phil Willems, "Heating Beam Pattern Optical Design CO2 Laser Thermal Compensation Bench", LIGO Document T040057-00
5. David Ottaway, "Design Requirements for the TCS Interface Board", LIGO Document E040320-00-D
6. Guido Mueller, Qi-ze Shu, Rana Adhikari, D. B. Tanner, David Reitze, Daniel Sigg, Nergis Mavalvala and Jordan Camp, *Optics letters*, Volume 25(4), pp 266-268, 2000

2 System Overview and Description

2.1 Introduction

Originally the LIGO 1 Interferometer was designed to be a point design with respect to input power. The radius of curvature of the Recycling Mirror (RM) was ground to be to concave to match the effective curvature of the Input Test Masses (ITMs) when the instrument was hot. It was anticipated that power absorbed in the ITMs would create a thermal lens that would alter the effective radius of curvature of the ITM as seen from the power recycling cavity side such that it matched the recycling mirror. This relies on accurate knowledge of the absorption coefficients of the ITM substrates and coatings. These are poorly controlled parameters. It has been shown by practical experience that relying on this method to geometrically stabilize the power-recycling cavity is not robust. The Hanford 4K interferometer has been shown to absorb excess power in the substrates and hence achieves an optimum power-recycling cavity at only 2.5 Watts of input power. The Hanford 2K and Livingston Interferometers do not reach the optimum operating point with the designed six watts of input power. It was decided that a means of correcting this thermal lensing problem and lack of robustness with respect to input power would be required. The desirable properties of such a system were as follows:

1. Must not add displacement noise to the ITMs that is greater than ten times less than the SRD.
2. Is easily adaptable as new understanding of the interferometer is realized
3. Should not require a significant vacuum incursion to install as this would lead to significant down time to the instrument
4. Must me reliable
5. Must be able to correct for both under-heating and over-heating of the ITMs by 1.064um radiation absorption

Thermal compensation has already been studied extensively for application to Advanced LIGO by Ryan Lawrence [1,2]. Lawrence studied the case for thermal correction of spatially homogenous absorption of the 1.064 um light using a shielded ring heater with spectacular results. In addition to this the correction of spatially inhomogeneous absorption correction with a scanned CO2 laser system and feedback using Shack-Hartmann sensors was also studied. This demonstrated a reduction in 10 of the power scattered from a TEM_{00} mode due a point absorber. We chose to use a combination of these techniques to attempt to correct LIGO 1 distortions. Direct application of the shielded heater rings was not used because of the significant vacuum incursion time that would be required to install such a system and its lack of flexibility once installed. The scanning CO_2 laser system was originally not chosen because of the requirement to install Shack-Hartman sensors, which would have required significant vacuum incursion. Later it was found by Phil Willems that the displacement noise imposed on the test masses by a scanning CO_2 laser system would be significant. The solution that was settled upon was a staring CO_2 system that would image a heat pattern onto the ITMs. This system could be made to correct either excessive heating or under-heating by simply changing the masks that were used to create/ the heat pattern. A basic concept schematic is shown in Figure 1. A complete schematic of the CO_2 imaging benches is included in Appendix 1.

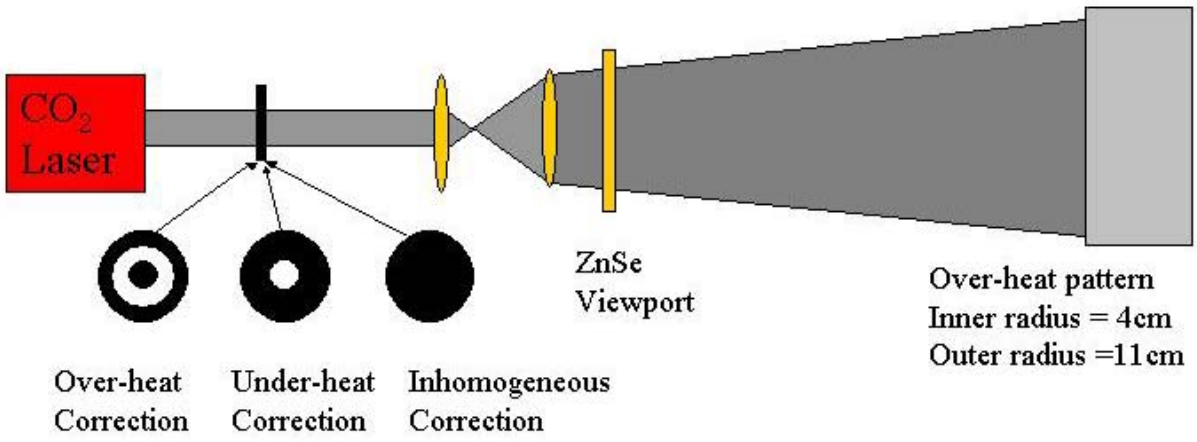

Figure 2-1Basic Schematic of the Thermal Compensation Design

2.2 Detailed Description of the Initial LIGO TCS system

The thermal compensation system consisted on the installing the following components:

1. ZnSe viewports
2. Camera housings that contained the top periscope mirror and large aperture zoom camera
3. Optical Imaging System mounted on a horizontal optical table

The most convenient viewports to inject the heating pattern though are located a distance of approximately 30m away from the ITMs, adjacent to the spool pieces. Due to the short absorption depth in of 10.6 um light in fused silica, ZnSe viewports were required. It is prohibitively expensive to get these viewports in large diameter windows. Hence the maximum diameter viewport that we could use was 2.5 inches clear aperture. The maximum resolvable feature on the ITM is given by:

$$\Delta x = 1.22 \frac{L\lambda}{D}$$

where L is the distance from the viewport to the optic, λ is the wavelength of light used (10.6 um) and D is the limiting aperture in this case the viewport. With these values the maximum feature that can be successfully resolved on the optic is 6 mm. Given this limitation, it was decided that this aperture must be the limiting aperture for the system. Further it was decided that the imaging system that images the mask plane onto the ITM must be diffraction limited so as not to further degrade this resolution limit.

An optical layout for the CO_2 table is included in Appendix 1. A complete parts list is available in reference 4.

2.3 The CO_2 Laser Projector

A detailed mathematical description of the TCS imaging system is described in reference 4, a qualitative summary is included here for completeness.

2.3.1 The CO_2 Laser

The laser that is used is an RF excited Merit-S Model CO_2 laser manufactured by Access Laser Company. The laser was chosen because of its proven ability to not line hop over extended periods during normal operation. It has a maximum output power of 8 Watts. The laser and its power supply are water cooled for improved reliability and elimination of fan noise. A purpose made chiller unit has been designed and built which combines the requirements of tight temperature control and low acoustic and RFI emissions. A description of this is covered in a separate document.

2.3.2 CO_2 Laser Power Control

The direct control of the power output of a CO_2 laser is only realizable though changes to the laser duty cycle. For noise reasons this method of power control is unacceptable and the laser must run

in CW mode. Therefore it is necessary to use an external form of power regulation to achieve the desired optical power level. Two types of power control have been implemented on the TCS system, namely: Accousto-Optic Modulator (AOM) power control (2K Interferometer) and Rotation of a polarizer (4K Interferometer at Livingston and Hanford).

For the initial installation on the 4K Interferometer at Hanford, we used an AOM to control the power. This was thought to be the preferred method of laser control because it gave us continuous control with a wide bandwidth, which we thought would be useful for intensity stabilization if required. In the later installations we switched to the slower method of polarizer rotation to give us control over the power. This was done for a couple of reasons, firstly the AOM was found to distort the laser beam significantly when high RF fields were used, thereby limiting the available optical power. Secondly, the intensity noise on the lasers was found to be at a sufficiently low level that active stabilization was deemed to be unnecessary (See Section 3.2 on Noise). The Hanford 4K which needs higher power compensation, was retrofitted with rotating polarizer light control and the AOMs were fitted to the Hanford 2K TCS system.

2.3.3 Beam Expansion and AOM matching

Lenses L7 and L8 are used to expand the beam exiting the laser such that it is the correct size to match into the AOMs.

2.3.4 Further Beam Expansion and Pattern Generation

It was decided that the best pattern for heating the center of the optics in the under-heat case is a Gaussian profile of identical size to the 1.064 um spot. It was also decided that it would be best if the central heating spot is independent of the input beam parameters.

The generation of the Gaussian profile central heating pattern is done, by clipping the beam with a mask consisting of a central hole. This flat top profile is then Fourier transformed into a Bessel function by L1. At the Fourier transform plane a fixed aperture is positioned with a diameter equal to the first Bessel function minimum. This creates a beam that is an excellent approximation to a Gaussian beam profile. L2 then performs another Fourier transform on the Gaussian profile to position it at the same location as the annulus mask.

When the central mask is not in place the beam is focused to considerably smaller spot size at the location of the fixed aperture and is hence not affected by it. In this case lenses L1 and L2 simply expand the beam such that it overfills the Annulus Mask. The plane where the annulus mask sits is imaged onto the ITM with the rest of the imaging system.

The lens L2M simply focuses the ray bundle incident on the annulus mask such that any additional power losses due to clipping on apertures down stream are insignificant.

2.3.5 The Imaging Telescope and the Periscope

The imaging telescope consists of three bean shaping elements, namely L3, L4 and M6. L3 creates a conjugate image plane for the annulus mask at infinity. This enables the telescope to be focused using L4 without changing the size of the image. M6 is a 6-inch diameter gold coated parabolic mirror. This was found to be necessary to prevent spherical aberration from significantly degrading the quality of the image. We use only a 2.5-inch, off-centered section of the mirror.

The mirror M7 is an elliptical shaped flat mirror that forms a periscope with another mirror of the same type that is located in the box housing the camera.

2.3.6 The Aiming Laser

The aiming laser is used to overlap a cross hairs pattern onto the projected heating pattern. This cross hair pattern is wide enough that they fall on the suspension cage of the ITM. The wide aperture camera mounted in the camera box is used to view the alignment cross hairs on the suspension cage. The aiming laser has a wavelength of 632 nm and an output power of 5mW. It is clearly shown on the optical layout. Lenses L5 and L6 are used to focus the aiming laser at the location of the test mass. It is combined onto the CO_2 laser beam using a dichroic mirror labeled as BS1.

3 TCS System Results

3.1 Beam Patterns

The heating patterns were measured by projecting the pattern onto a white target located outside of the vacuum system and 30 m from the viewport. This was

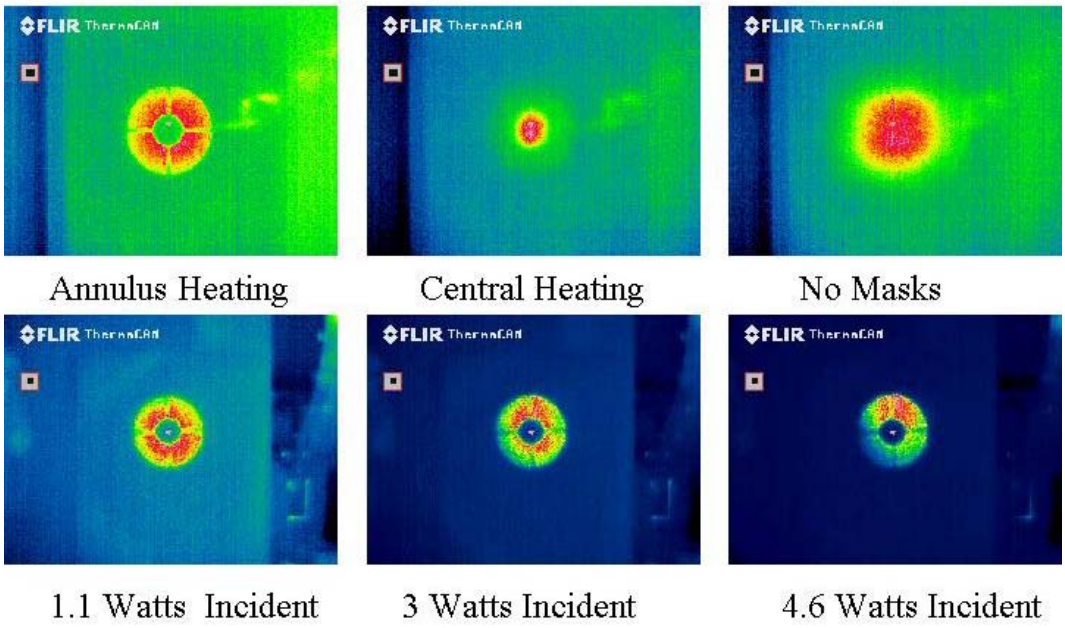

Figure 3-1 Heating profiles measured using a thermal imaging camera during the commissioning of the Hanford 4 K TCS. At this time this system used the AOM power control.

3.2 Noise Models

Mike Zucker analyzed the effect of central heating of the ITMs using a CO_2 laser (3) for the case of both front surface and back surface heating. The noise mechanisms that were studied were:

1. Dynamic changes in the substrate leading to changes in the Michelson degree of freedom. This is the same for either front face heating
2. Changes in the arm cavity length due to thermally induced expansions of the optic. Not surprisingly this is appreciably worse for front face heating than back face heating
3. Radiation pressure modulation of the arm cavity length.

For the LIGO 1 case, with front surface heating the dominant noise mechanism is the second one. The predicted effect of CO_2 laser intensity noise on the displacement noise of the interferometer is given by:

$$x_{HR}(f) \approx 10^{-20} \frac{m}{\sqrt{Hz}} \left(\frac{150Hz}{f} \right) \left(\frac{\langle P_A \rangle}{25mW} \right) \left(\frac{RIN}{4.10^{-6} Hz^{-1/2}} \right)$$

Where RIN is the relative intensity noise of the CO_2 laser, $<P_A>$ is the power absorbed in the substrates and f is the modulation frequency.

Stefan Ballmer and Cheryl Vorvick measured the transfer function from the heating laser modulation to test mass displacement for both annulus and central heating. The results are shown as Figure 3-2

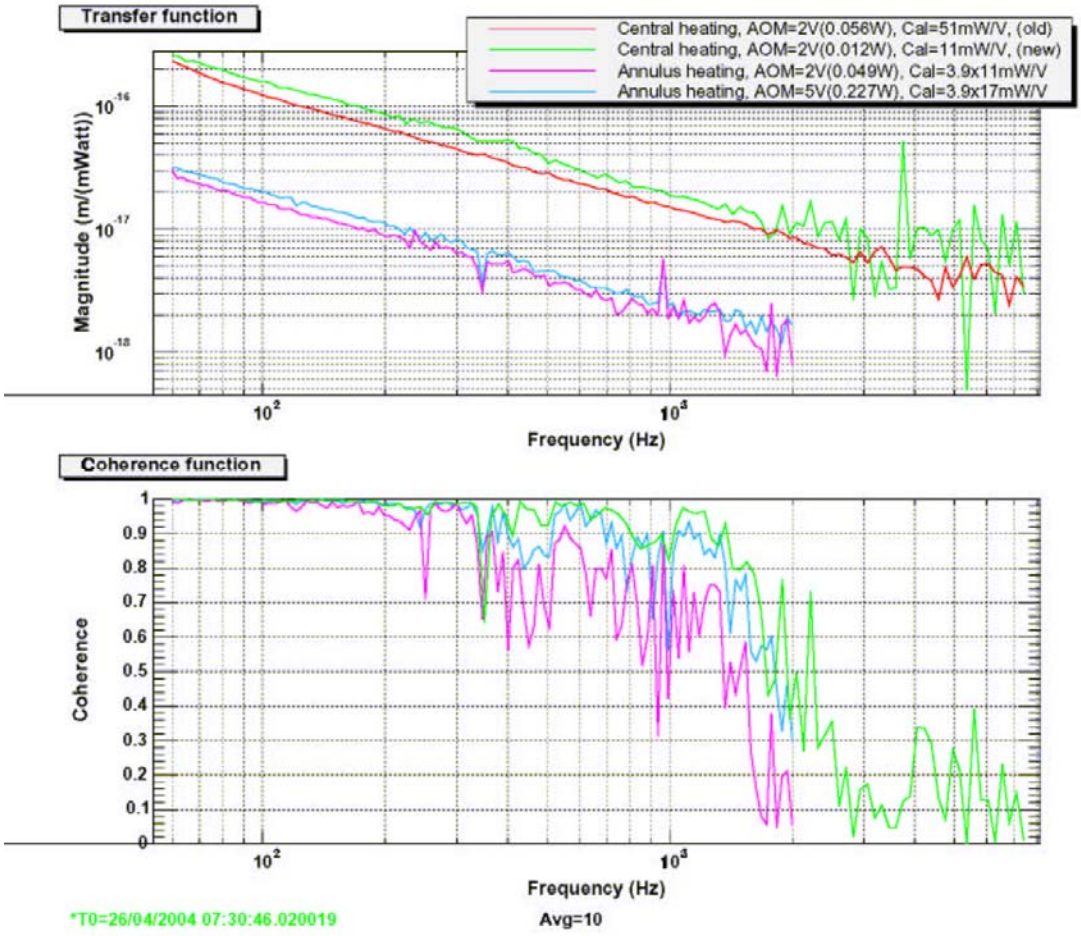

Figure 3-2 Transfer function between modulation of heating laser power and displacement noise of ITM

The measurement and the theory agree exceptionally well at 150 Hz. The transfer function of annulus heating on displacement noise is a factor of 10 below that of central heating. This is fortunate as appreciably more power is required for annulus heating. The transfer function for annulus heating is more difficult to predict theoretically and at present we do not have a theoretical model to compare the experimental results to.

The intensity noise spectra of the CO_2 lasers have been measured and a typical intensity noise spectra is shown as Figure 3-3

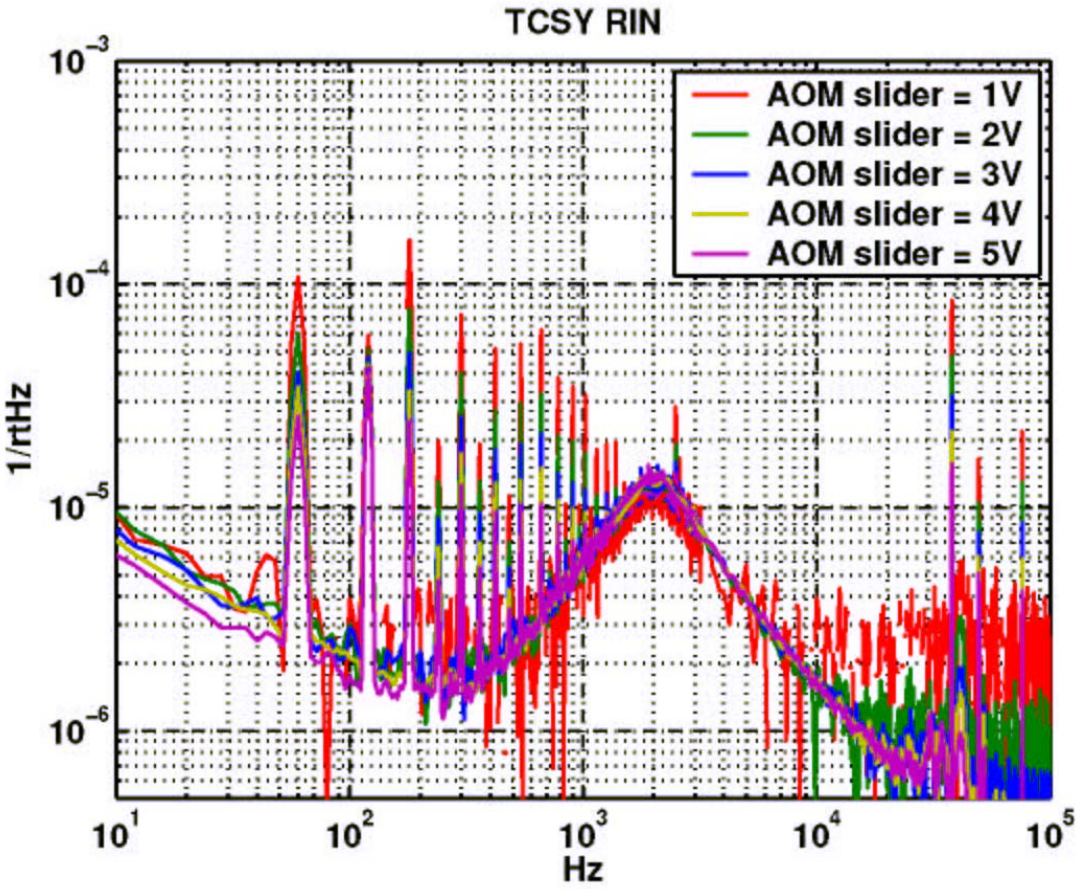

Figure 3-3 Typical Relative Intensity Noise of the Access Laser CO2 Lasers

The results of the measured transfer function and the intensity noise spectra of the CO_2 laser were combined to predict the impact on displacement noise sensitivity of the interferometer. The results for 90 mW of central heating are shown in Figure 3-4

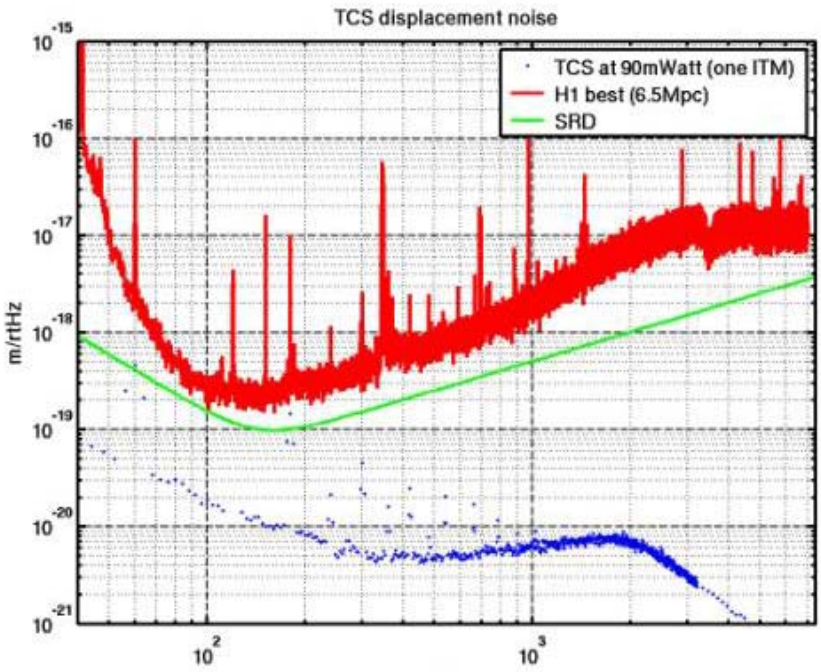

Figure 3-4 Predicted Impact of heater laser central heating with 90 mW of incident power

4 Theoretical Calculations

4.1 Homogenous Absorption Profiles

A model adapted from one originally written by Lawrence was adapted to predict the effect of the TCS on LIGO1 ITMs. The model can also be used to predict the effect of absorption of 1.064 um light on the test masses. These profiles are included for completeness as Figure 4-1, Figure 4-2, Figure 4-3 and Figure 4-4. The code solves the 2 dimensional heatflow equation and thermo-elastic deformation equations.

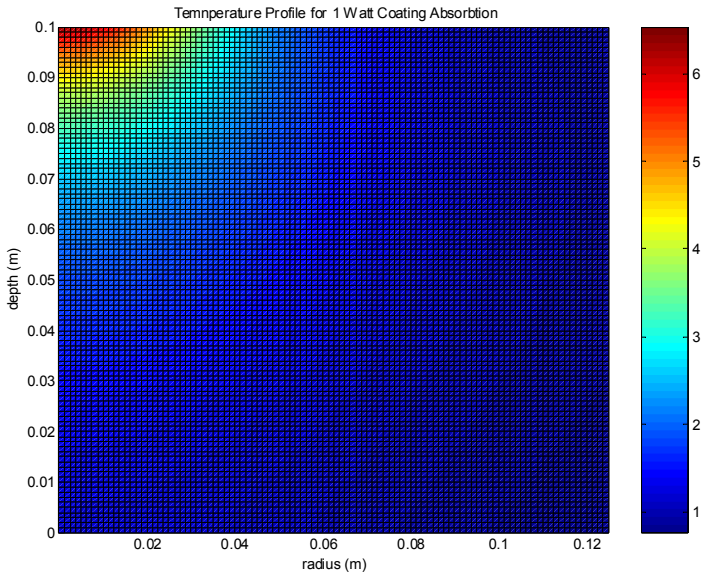

Figure 4-1 Temperature Profile for 1 Watt of Coating Absorption

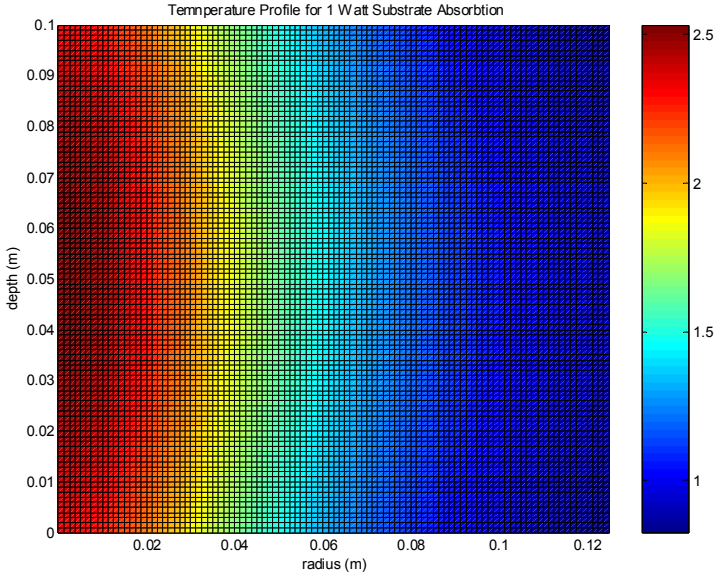

Figure 4-2 Temperature Profile for 1 Watt of Substrate Absorption

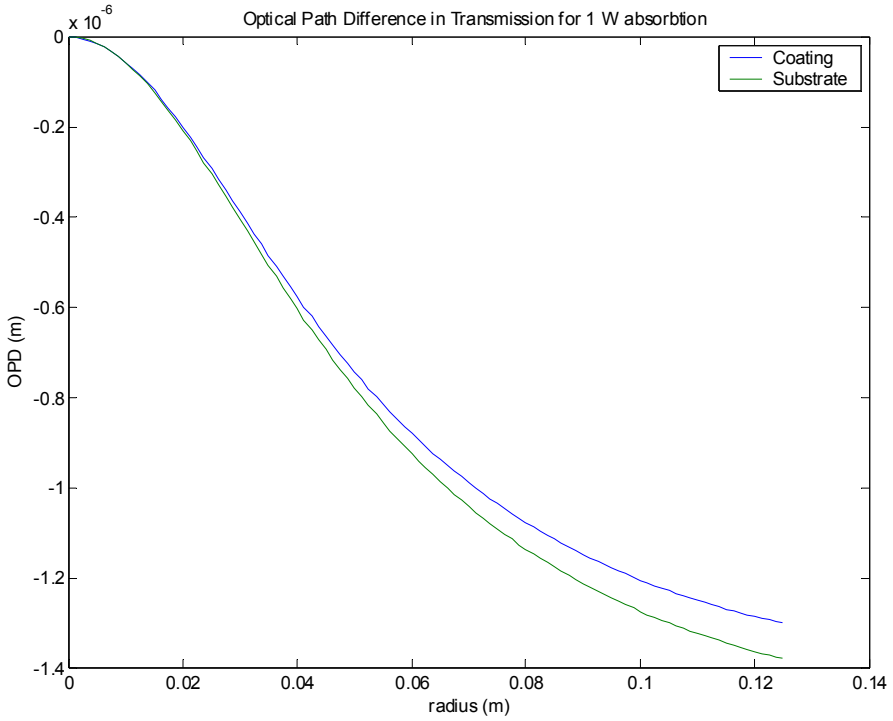

Figure 4-3 OPD in Transmission with 1 Watt of Absorption

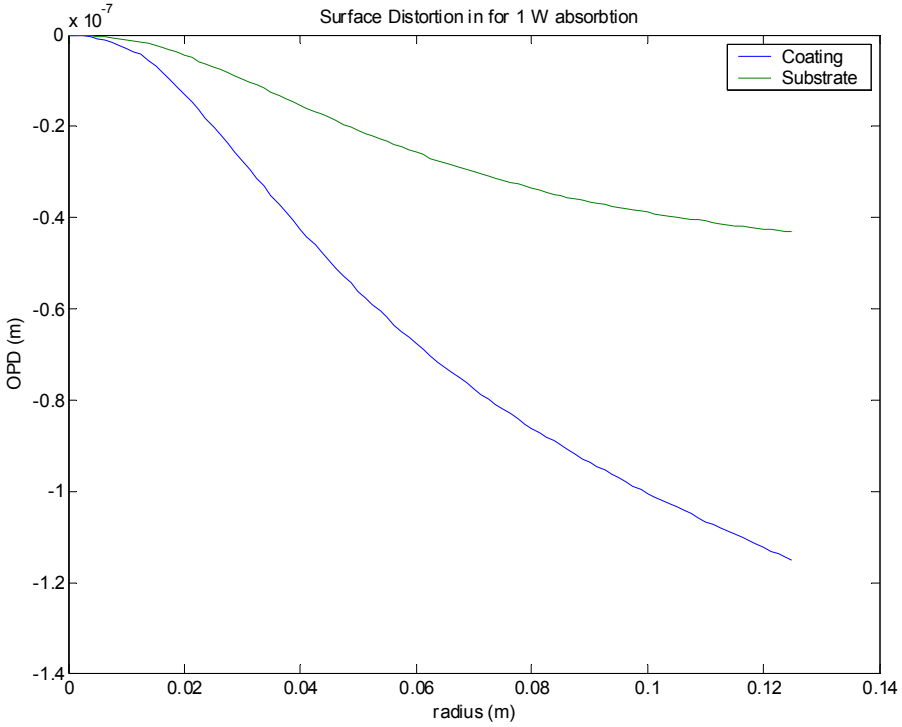

Figure 4-4 Surface Distortion for 1 Watt of Absorption

4.2 Calculated TCS Profiles

The calculate heat profile in Figure 4-5 is for case of one watt of annulus heating with an inner radius of 4 cm and an outer radius of 12cm. In addition to this the mask is illuminated with a Gaussian beam of spot size of 12 cm.

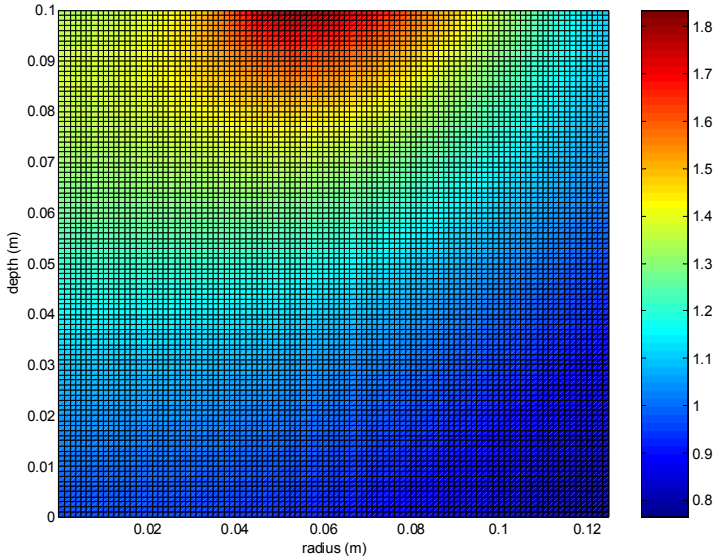

Figure 4-5 Temperature Profile for 1 Watt of Annulus TCS with a 4cm inner radius

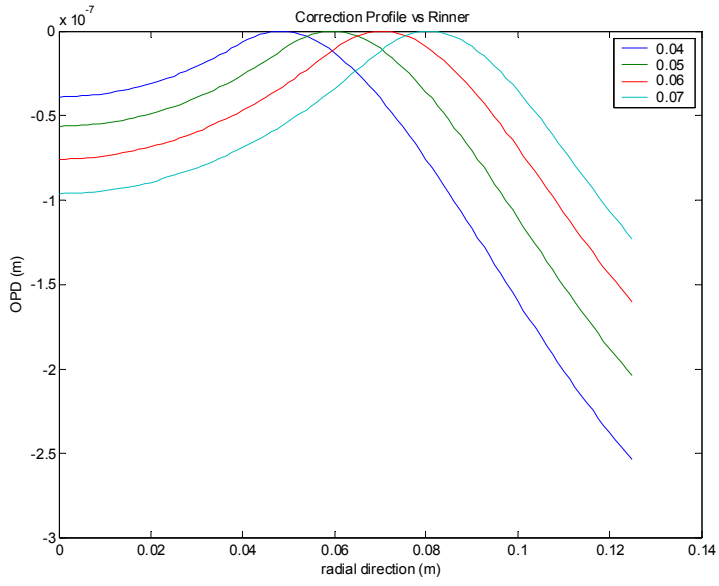

Figure 4-6 OPD Profile for various inner annulus radii

4.3 Optimization of the TCS System

For the first installation of TCS a binary mask was chosen. At the time it was known that the IFO reached optimum heating point with 2.5 Watts incident on the IFO. The interferometer high power operating state called for 6 Watts of power. For this reason the initial masks were designed for correcting the situation when the optics over heat by a factor of 2. The masks were optimized for the inner annulus radius and the outer annulus radius. The results are given in Figure 4-7 and 4-8.

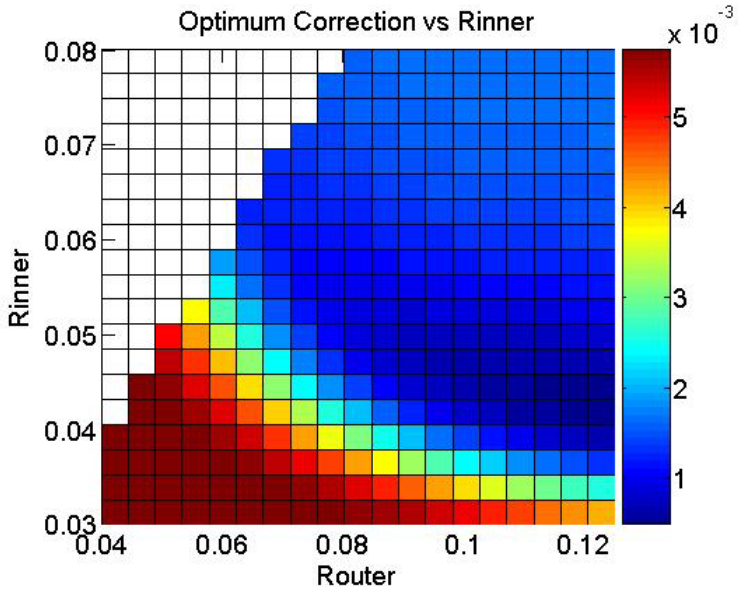

4-7 Optimum Correction with varying Rinner and Router for an overheat case of a factor of 2

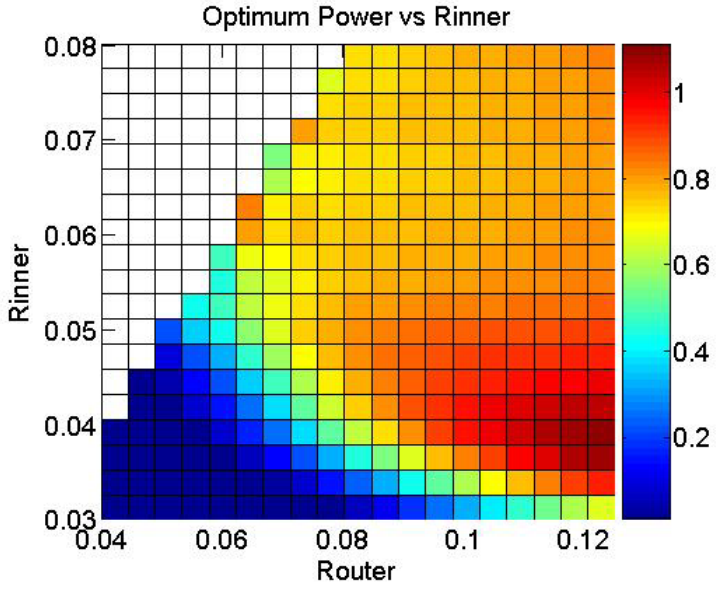

4-8 Power required for best possible correction when optics are overheated by a factor of 2

4.4 Limits on the Binary Mask TCS Performance

It has been found that in the Hanford 4K IFO the ITMX is absorbing twice as much power as the ITMY. This is putting a considerable strain on the x-arm TCS system for this IFO. To achieve 6 Watts incident on the MC the ITMX will overheat by a factor of 4. To achieve the SRD slightly more power than this will be required. A higher power TCS laser on the x-arm will be installed. A quick investigation on how the TCS will perform under this increased power was performed. The results are as follows:

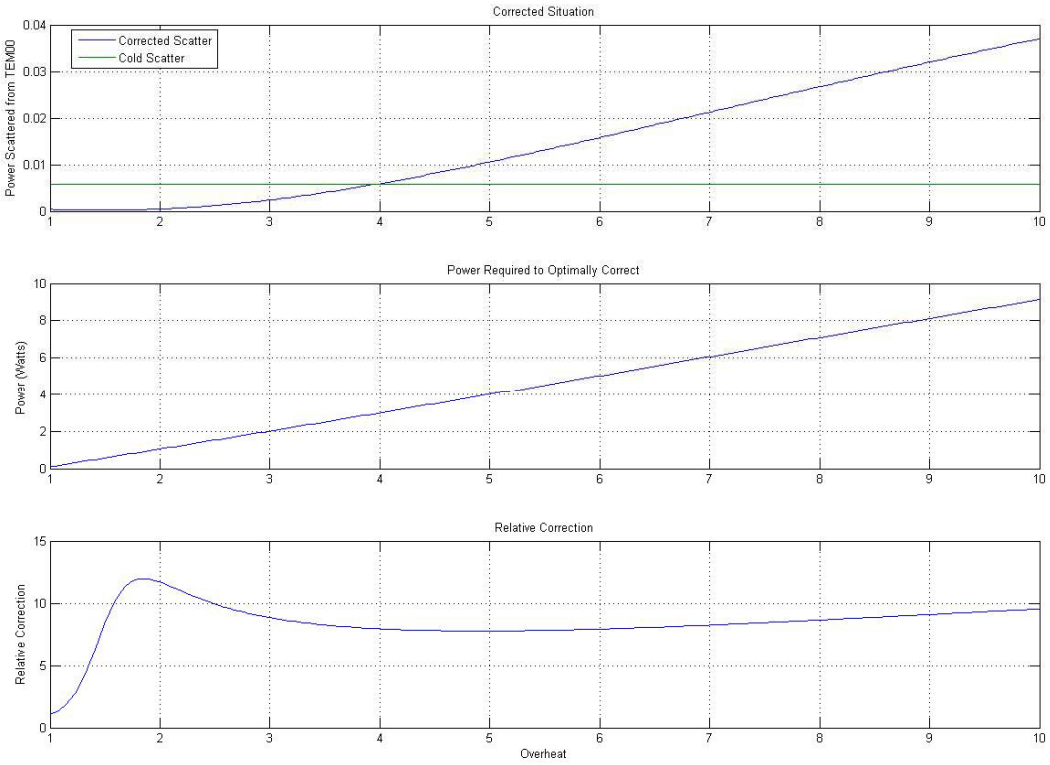

Figure 4-9 The effect of increased 1.064 micron absorption on TCS performance. The change in the scatter from at TEM00 mode is compared to the scatter from a cold ITM (Top plot). The power required in the annulus heating is shown (Middle plot). The improvement due to TCS is shown in the bottom plot

Figure 4-9 clearly illustrates that the TCS binary masks will be insufficient when the overheat factor reaches a factor of 3. This is not because TCS correction is degrading it is just that the initial distortions are getting worse and hence a more precise correction is required. Therefore to gain full benefit from the higher power CO2 lasers it will be necessary to reshape heating profile. The current TCS system allows this to be done by making masks that consist of sub-resolution holes. The current TCS system resolves objects that are 0.5 mm in diameter on the mask plane. Therefore

if masks are manufactured that consist of 0.1 mm holes then the intensity profile can be changed by increasing the density of sub-resolution holes on the mask plane. If greater range is required the resolution of the telescope can be deliberately reduced. Lawrence et al. showed two orders of magnitude improvement in the scattered light from an over heated optic using shielded ring compensation (1, 2). Any correction pattern that can be demonstrated using a shielded ring compensation system can be in principle created using the current TCS system with the correct mask selection. At the time of writing Phil Willems is currently designing such masks.

4.5 Time Dependent Behavior of TCS

Stefan Ballmer noticed that the effectiveness of the annulus correction decreased over a period of many hours. A time dependent finite element model was written to model the time dependent profile of the annulus heating. The result is shown as Figure 4-10

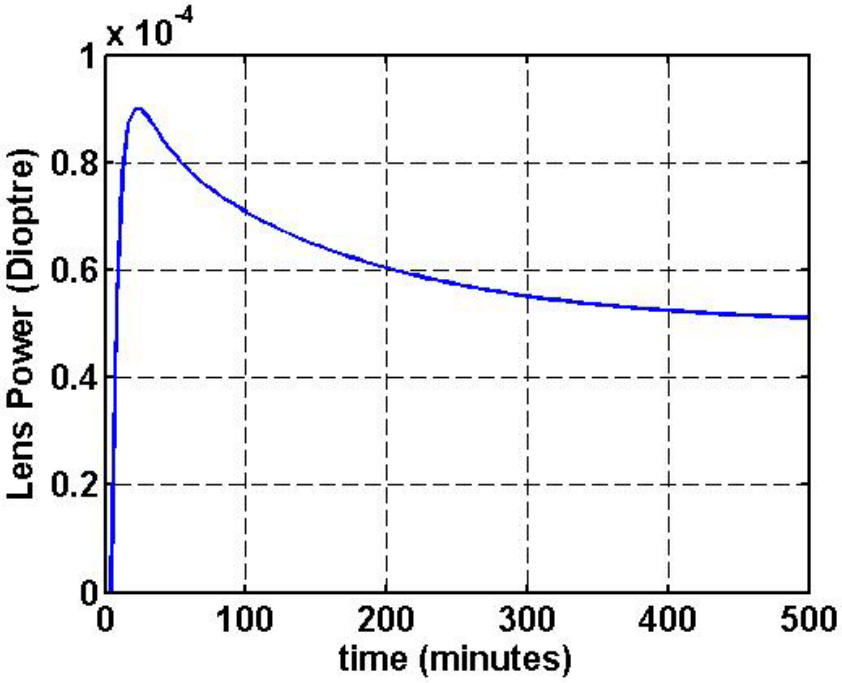

4-10 Time dependence of the power of the thermal correction due to annulus heating

Figure 4-10 clearly shows that the effectiveness of annulus compensation decreases with time. Fortunately all of the design modeling was done in the steady state case. This reduction is due to the fact that when annulus correction is applied the heat is applied exactly where the correction is needed. As time progresses the heat flows into the center of the optic increasing its temperature and decreasing the effectiveness of the annulus correction.

5 TCS Servo Control

5.1 Introduction

The time dependence of the induced thermal lens (time constant ~ 4 hours) meant that a simple "set and leave" operation was no longer feasible since the typical lock duration is not much larger than the thermal time constant. It became necessary to adjust the applied TCS power dynamically in

order to keep the interferometer at the optimal recycling gain. In other words: yet another servo was required.

5.2 Error Signals

To implement the servo we needed a simple way to read out the thermal state of the interferometer. Furthermore this signal has to be linear at least in a region around the optimal recycling gain point. As a first attempt we tried to use the spiricon to measure the antisymmetric (AS) port spot size. The AS port was chosen because it is dominated by the sideband fields. However the spot size fluctuations due to alignment instabilities were too large to get a clean error signal.

The signal that was ultimately used is the wavefront shape of the 1-omega beat of sideband and carrier in the pick-off (PO) port. The mode shape of the sideband the marginally stable recycling cavity is strongly dependent on the thermal lens in the ITM's, while the carrier is mostly dictated by the arms. Thus, in 1st order perturbation, the radial dependence of the beat wave front is given by the 1st Laguerre polynomial (1-2r2/w2), i.e. the "bull's eye" mode. We therefore needed a radial wave front sensor.

Since we actually have two TCS systems (on ITMX and ITMY) and hence two actuation degrees of freedom, we need a 2nd error signal. It was found experimentally that the AS_I signal is usable for that purpose.

Later Hiro Yamamoto pointed out that this dependence is expected if the wavefronts of the 2 arms are not well matched (G050061-E).

5.3 Sensor

Fortunately, back in 1999, the University of Florida developed such a wave front sensor (5) and all we had to do is de-dust it and retune its tank circuits. This Bull's eye detector consists of a central active segment surrounded by 3 additional active segments arranged in a ring. Its node, i.e. the division between central and outer segments, is at a radius of 1mm. Thus we had to aim for a beam radius w of ~1.4mm.

To get a good signal the Bull's eye detector should be in the same Gouy phase as the recycling cavity. However Bill Kells calculated that using a simple f~=1m lens to focus the beam and placing the detector at the w=1.4mm spot in front of the focus leads only to a Gouy phase advance of approximately 5 degrees, which is acceptable.

5.4 Implementation

The Bull's eye detector was installed on the POB port of the H1 interferometer and uses the electronic slots of the (not used) wave front sensor 5. The front end ASC and LSC code were modified somewhat: The WFS5 filter module is now independent of the WFS master gain. A mixing matrix for the 4 AS_I signals including a filter module for the combined signal was added.

This new AS_I filter module and the WFS5_PIT filter module were used as anti-alias filters. The actual servo was implemented as a stand-alone module running on a sun machine at a sampling rate of 1Hz and using EPICS channels as inputs and outputs.

The data flow of this servo module is shown in Figure 5.1. Some logic to automatically choose central or annulus mask was added, but in practice never used since a mask flip introduces a transient and since in regular operation changing the mask was never required. Typically the input matrix was chosen to be diagonal so the control was done in the common/differential basis. The control filter was chosen to get a 1/f loop shape: Pole at 0Hz and 0.1Hz (roll off), zero at 1/10min to compensate the thermal pole. Figure 5.2 shows the expected thermal transfer function for central and annulus heating as obtained by the time-step finite element model. It confirms that the above filter choice should roughly lead to the desired 1/f shape.

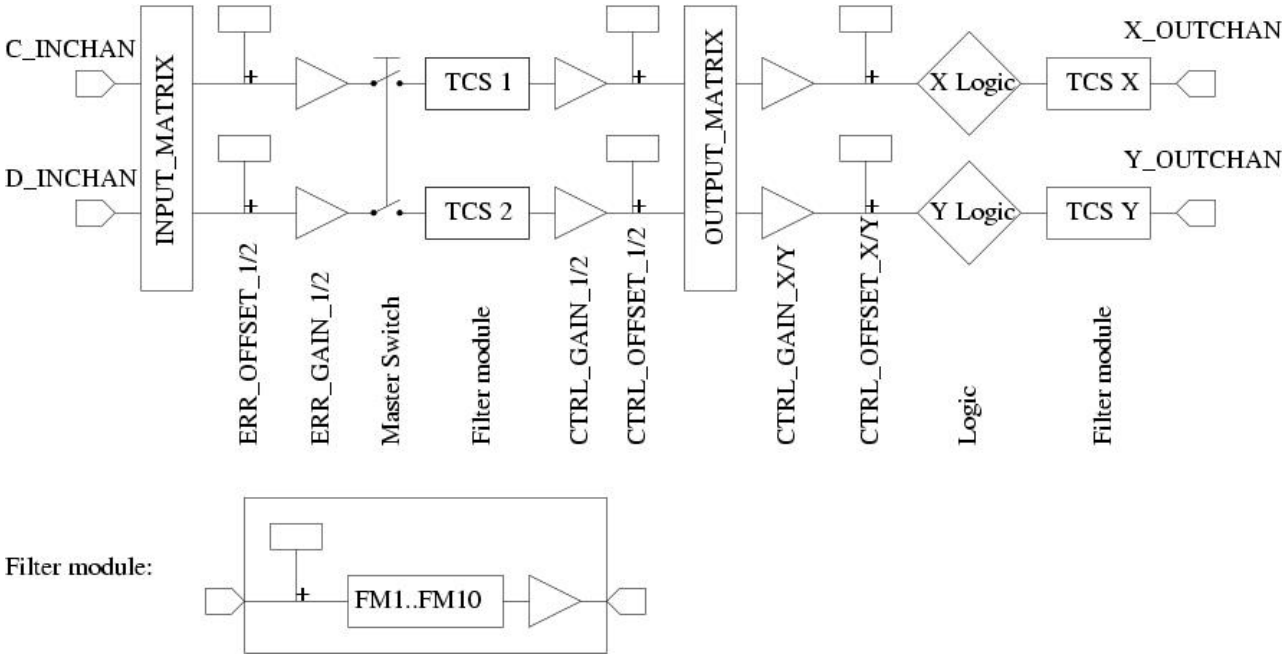

5-1 Block diagram of the TCS servo system

In practice it turned out to be favorable to establish a gain hierarchy and run the common servo at a higher gain.

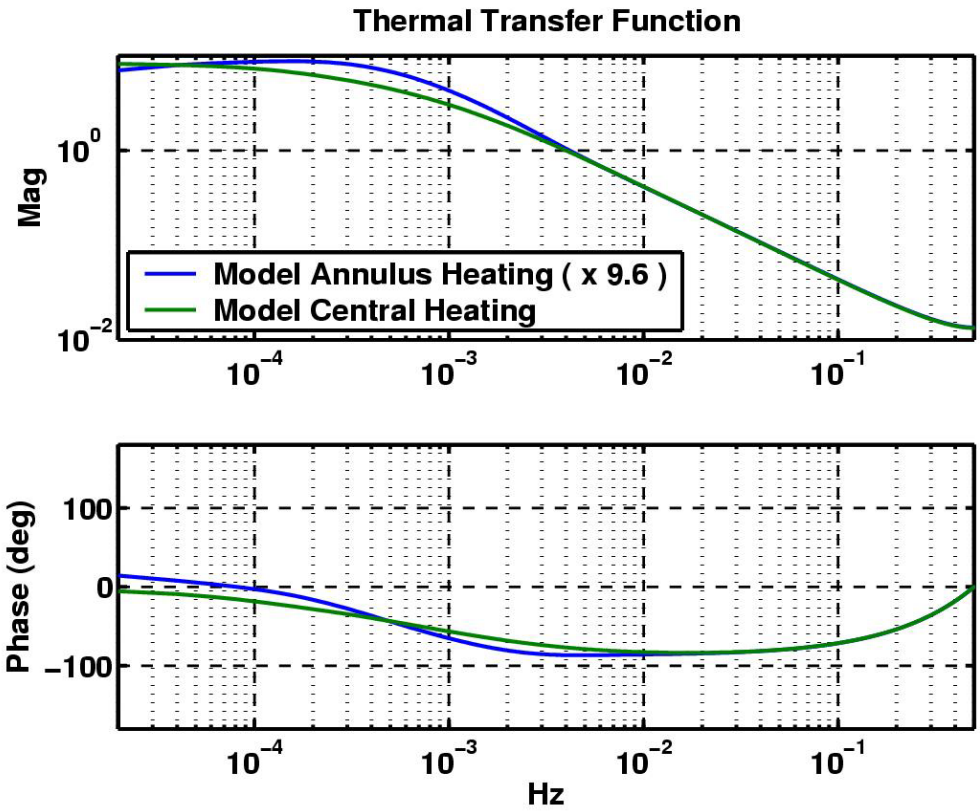

5-2 Modeled transfer function for annulus and central heating applied power to lens gained.

Appendix 1. Schematic of 4K TCS Layout